Reference optimisation of uncertain offshore hybrid power systems with multi-stage nonlinear model predictive control*

Kiet Tuan Hoang[1], Brage Rugstad Knudsen[2], Lars Imsland[1]

Abstract— **This paper presents a modified multi-stage economic nonlinear model predictive controller (M-ENMPC) for reference optimisation of isolated, uncertain offshore hybrid power systems (OHPSs). These systems require control strategies that can handle significant stochastic disturbances in exogenous power demand and wind, given uncertain forecasts of the disturbances. An M-ENMPC modified with a certainty horizon is formulated to hande uncertain forecasts of these disturbances for reference optimisation of OHPSs. The certainty horizon models the increase in uncertainty of forecasts with time to decrease the cost in the M-ENMPC. Monte Carlo simulations with different realisations of the considered disturbances show that explicitly considering scenarios of the disturbances with the M-ENMPC can decrease greenhouse gas (GHG) emissions by operating the gas turbines in the hybrid power system more efficiently while achieving an acceptable satisfaction of the exogenous power demand. Furthermore, the Monte Carlo simulations show that using the modified M-ENMPC decreases the average computational time by 17% compared with the conventional M-ENMPC from literature.**

I. INTRODUCTION

Complex industrial systems are often handled by decomposing the decision-making process into a hierarchy of different time-scales [1]. Reference generation, the transfer of decisions from an upper to a lower level, is vital in these systems to take advantage of a priori knowledge. In its simplest form, a high-level reference generator can be used to generate a reference for some low-level PID controllers to track given knowledge of some forecasts of disturbances (see, for example, [2]). In the case of isolated, hybrid power systems, the disturbance can occur as an uncertain forecast of wind power production (due to uncertain meteorological forecasts of the wind speed), which then can be used to coordinate other deterministic power suppliers and power storage systems [3]. However, due to its intermittent nature, generating references for energy infrastructure with high penetration of renewable energy sources is non-trivial. Significant deviations between the actual and the predicted wind power production may decrease the total performance of such systems which are dependent on optimal coordination between power suppliers, power storage systems, and exogenous power demand.

Several ways of reference generation for deterministic systems, where references are computed based on an optimal state prediction, have already been investigated. In process control, real-time optimisers (RTOs) are widespread due to their low computational demand as the references are generated based on steady-state dynamics [4]. Extensions to capture transient dynamics can be found in economic model predictive control (EMPC), see for example [2], [5], [6].

In practice, a certainty-equivalent EMPC (CE-EMPC) approach is commonly used in case of significant disturbances. To explicitly consider the uncertainty, both stochastic and robust approaches have been explored in the literature. Robust methods prevents constraint violations under uncertainty by relying on the maximum and minimum formulation of some bounded uncertainties, to represents all realisations of the uncertainty [7]. In contrast, a stochastic approach allows for some constraint violation by neglecting improbable realisations of the disturbances for some increased performance [8].

Here, a subcategory of stochastic economic nonlinear model predictive control (ENMPC), the M-ENMPC with continuous-time uncertainties in power generation and demand, is explored, for reference generation of OHPSs consisting of intermittent offshore wind energy that must be coordinated with other power systems such as batteries and gas turbine generators to achieve optimal performance [3]. The M-ENMPC is an approximate method of scenario-based optimisation that handles, additionally to the nominal case of the disturbance, also the minimum and maximum case realisation of the disturbances to prevent constraint violation and improve performance [9]. The M-ENMPC has been applied to many different applications, such as for the semi-batch polymerisation reactor [9], obstacle avoidance in autonomous vehicles [10], and daily production optimisation in petroleum production [11].

The novelty of this paper is twofold. First, an M-ENMPC is proposed to handle uncertainty in forecasts of power production (uncertain offshore wind) and demand in an OHPS by considering approximate minimum and maximum scenarios of the disturbances (which are assumed known for simplicity). The main point is to show how considering uncertainty in a gas turbine, wind turbine, and battery configuration can lead to decreased GHG emissions with more efficient use of the gas turbine while robustly utilising the battery to satisfy some uncertain power demand. Secondly, a certainty horizon is proposed to decrease the computational cost of the M-ENMPC. The certainty horizon is motivated by the decreasing accuracy of forecasts one can expect in such systems. For simplicity, the references are assumed to be perfectly tracked by some low-level controllers.

The remainder of the paper is structured as follows:

* This work has received financial support from the Research Council of Norway through PETROSENTER LowEmission (project code 296207).

[1] K.T. Hoang and L. Imsland are with the Department of Engineering Cybernetics, Norwegian University of Science and Technology, Trondheim, Norway, {kiet.t.hoang,lars.imsland}@ntnu.no

[2] B.R. Knudsen is with SINTEF Energy Research, Trondheim, Norway, brage.knudsen@sintef.no

Section II presents the OHPS, followed by a general formulation for the modified M-ENMPC in Section III. In Section IV, a simulation study is presented using the proposed methodology for an OHPS, given different realisations of the disturbances with Monte Carlo simulations. The paper will conclude with Sections V and VI.

II. OFFSHORE HYBRID POWER SYSTEMS

OHPSs, such as the one illustrated in Fig. 1, provide a means to decarbonise the energy supply on the Northern Continental Shelf by increasing the penetration of renewable energy into the offshore energy infrastructure, which today consists of primarily gas turbines [12]. Control solutions that efficiently and robustly handle uncertainties in forecasts of wind power generation (due to uncertain wind speed forecasts) and exogenous power demand is therefore essential for power system stability and efficiency, see Fig. 1. This exogenous power demand can stem from decentralised power sinks, such as maritime transport, green hydrogen, aquaculture, or petroleum production [13].

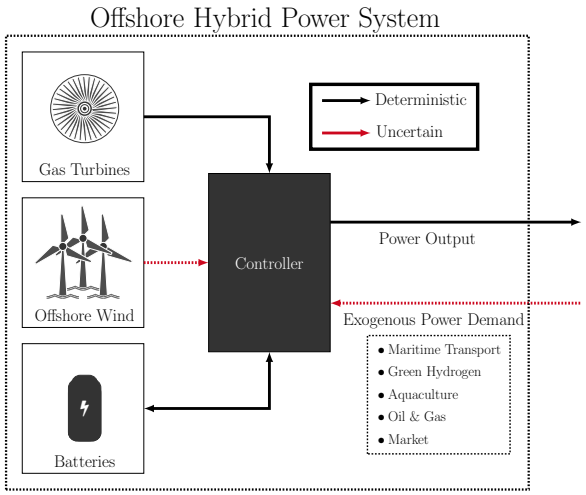

Fig. 1. An illustration of offshore hybrid power systems with offshore wind energy, gas turbines, and batteries.

Generally, optimal operation of production and storage in the OHPS is vital if the power demand is significantly greater than the maximum gas turbine power output and the current wind power. An intelligent controller can preemptively charge the battery in advance and allow the OHPS to act more robustly regarding the power demand [3]. Furthermore, a vital controller aim for such a system is ultimately to lower the emitted GHG emissions. Lower GHG emissions can be achieved through 1) maximising the wind power by storing excess wind power in the battery or 2) by operating the gas turbine more efficiently and lowering the total GHG emissions [14].

A. Modeling of Offshore Hybrid Power System

The isolated nonlinear OHPS considered in this paper consists of three subsystems: a gas turbine generator (GTG) system, a wind turbine generator (WTG) system, and a battery (Bat) system with the following system dynamics $f : \mathbb{R}^{n_x} \times \mathbb{R}^{n_u} \times \mathbb{R}^{n_d} \to \mathbb{R}^{n_x}$ and measurement function $h : \mathbb{R}^{n_x} \times \mathbb{R}^{n_u} \times \mathbb{R}^{n_d} \to \mathbb{R}^{n_y}$ (refer to [3] and the references herein for further information on the modelling and assumptions)

$$\begin{aligned} x_{k+1} &= f\left(x_k, u_k, d_k\right) \\ y_k &= h\left(x_k, u_k, d_k\right), \end{aligned} \tag{1}$$

where system state vector $x = [V_{\text{gtg}}, P_{\text{gtg}}, \omega_{\text{wtg}}, M_{\text{wtg,gen}}, \text{SOC}_{\text{bat}}]^\top \in \mathbb{R}^{n_x}$, system input vector $u = [T_{\text{gtg}}, \beta_{\text{wtg}}, I_{\text{bat}}]^\top \in \mathbb{R}^{n_u}$, system disturbance vector $d = [\text{v}_{\text{wind}}, P_{\text{demand}}]^\top \in \mathbb{R}^{n_d}$, and system output vector $y = [P_{\text{gtg}}, P_{\text{wtg}}, \text{SOC}_{\text{bat}}, \omega_{\text{wtg}}]^\top \in \mathbb{R}^{n_y}$. In which, V_{gtg} [pu] and P_{gtg} [kW] describe the GTG fuel flow and power output, ω_{wtg} [$\text{rad}\,\text{s}^{-1}$] and $M_{\text{wtg,gen}}$ [$\text{N}\,\text{m}$] describe the rotational speed of the wind turbine and the WTG generator torque, SOC_{bat} [%] describes the battery state of charge, T_{gtg} [pu] describes the GTG throttle, β_{wtg} [deg] describes the WTG blade pitch, I_{bat} [A] describes the battery current, v_{wind} [$\text{m}\,\text{s}^{-1}$] and P_{demand} describe the average WTG rotor wind speed and the total power demand, and P_{wtg} [kW] describes the WTG power output.

B. Control Objective

The control objective of this constrained OHPS is to (in decreasing order of importance):

1) Satisfy the uncertain total power demand
2) Maximise WTG power to reduce GHG emissions
3) Maximise GTG efficiency to reduce GHG emissions
4) Minimise GTG power to reduce GHG emissions
5) Maximise the battery SOC for system flexibility
6) Minimise actuator effort

These control objectives (except for the satisfaction of the uncertain total power demand) can intuitively be formulated in terms of four cost functions terms θ_i

$$J_{\text{ohps}}(x, u, d) = \theta_{\text{wtg}} + \theta_{\text{gtg}} + \theta_{\text{bat}} + \theta_{\mathbf{u}} \tag{2}$$

$$\theta_{\text{wtg}} = K_{\text{wtg}}(P_{\text{wtg}} - P_{\text{wtg,max}})^2 \tag{3}$$

$$\theta_{\text{gtg}} = K_{\text{gtg},\eta}(\eta_{\text{gtg}} - \eta_{\text{gtg,max}})^2 + K_{\text{gtg},P} P_{\text{gtg}} \tag{4}$$

$$\theta_{\text{bat}} = -K_{\text{bat}} \text{SOC}_{\text{bat}} \tag{5}$$

$$\theta_{\mathbf{u}} = u^\top K_u u, \tag{6}$$

where K_i are positive constants or matrices to be tuned, $P_{\text{wtg,max}}$ is the maximum power output from the WTG, and η_{gtg} is a function that describes the efficiency of the GTG as a second-degree polynomial (adapted from [14] assuming a combined-cycle LM2500 turbine with α_i as fitted constants)

$$\eta_{\text{gtg}} = \begin{cases} \alpha_1 P_{\text{gtg}}^2 + \alpha_2 P_{\text{gtg}}, & \text{if } P_{\text{gtg}} \geq 0.01 P_{\text{gtg,max}}. \\ 0, & \text{otherwise.} \end{cases} \tag{7}$$

In general, there are two approaches for ensuring the satisfaction of exogenous power demands in constrained optimal control: 1) in the cost function with $\theta_P = P_{\text{demand}} - P_{\text{wtg}} - P_{\text{gtg}} - P_{\text{bat}}$, or 2) as a constraint

$$g_P = P_{\text{demand}} - P_{\text{wtg}} - P_{\text{gtg}} - P_{\text{bat}} = 0. \tag{8}$$

The methods considered in this paper use 2), formulated as a soft constraint to guarantee feasibility as there may

be scenarios where P_{demand} cannot be satisfied even with a perfect forecast of P_{demand} and v_{wind} (thus also P_{wtg}).

Remark 1: Only control objectives 1, 3, and 4 are chosen as key performance indicators (KPIs) for the simulation study as they are easily quantifiable. Objective 2 is omitted as it is assumed that P_{wtg} is maximised at every time step since the references are known with no measurement noise for the current time step, where the P_{demand} is never low enough that P_{wtg} has to be dissipated for grid stability.

Additionally, the amount of GHG emissions (measured in CO_2) is also used as a KPI and minimised indirectly with θ_{gtg} as it is more easily understood and combines control objectives 3 and 4, respectively. The total GHG emissions is in this paper computed as

$$\dot{m}_{\text{CO}_2} = \frac{\text{M}_{\text{CO}_2}}{\text{M}_{\text{CH}_4}} \dot{m}_{\text{CH}_4} = \frac{\text{M}_{\text{CO}_2}}{\text{M}_{\text{CH}_4}} \frac{P_{\text{gtg}}}{\eta_{\text{gtg}} \text{LHV}_{\text{CH}_4}}, \tag{9}$$

where M is the molecular weight [g/mole], $\dot{m}$ [kg/s] is the mass flow of reactant/product, and LHV is the lower heating value. Equation (9) is derived by assuming ideal, stoichiometric combustion of methane with air

$$\text{CH}_4 + 2(\text{O}_2 + 3.76\text{N}_2) \longrightarrow \text{CO}_2 + 2\text{H}_2\text{O} + 7.52\text{N}_2$$

III. OPTIMAL REFERENCE GENERATION WITH UNCERTAIN DISTURBANCES

The most common approach when using ENMPC is to ignore the uncertainty by relying on the certainty-equivalence (CE) property [15] even if this does not formally hold (Subsection III-A). A CE-ENMPC may therefore incur performance losses. To handle and exploit uncertainty information, the multi-stage variant from [9] is proposed for reference generation (Subsection III-B).

A. Baseline controller - Certainty-Equivalent approach

A CE-ENMPC formulates the control problem as an optimisation problem by considering future potential control actions using an imperfect disturbance value $\widehat{d}$. Commonly, the control law can be computed as a policy by solving a nonlinear program (NLP) in the form of [16]

$$\begin{aligned} \min_{x,u} \quad & \sum_{k=0}^{N_P} J_{\text{ohps}}\left(x_k, u_k, \widehat{d}_k\right) \\ \text{subject to:} \quad & x_{k+1} = f\left(x_k, u_k, \widehat{d}_k\right), \ \forall k \in [0, N_P] \\ & h_{\text{ineq}}\left(x_k, u_k, \widehat{d}_k\right) \leq 0, \ \forall k \in [0, N_P] \\ & g_{\text{eq}}\left(x_k, u_k, \widehat{d}_k\right) = 0, \ \forall k \in [0, N_P], \end{aligned} \tag{10}$$

where N_P is the prediction horizon, $J(\cdot)$ is the cumulative cost function from (2), $x_{k+1} = f(x_k, \cdots)$ are dynamic model constraints (the main cause of nonlinearity is due to the aerodynamics), $h_{\text{ineq}}(\cdot)$ and $g_{\text{eq}}(\cdot)$ are general vectors of inequality and equality constraints ($h_{\text{ineq}}(\cdot)$ and $g_{\text{eq}}(\cdot)$ relevant for the OHPS can be found in [3]), $\widehat{d}_k$ is the uncertain disturbance vector, $x = [x_1, ...x_{N_P}]$ and $u = [u_0, ...u_{N_P}]$ are the decision variables to be optimised, and x_1 is the optimal next step reference for the lower level.

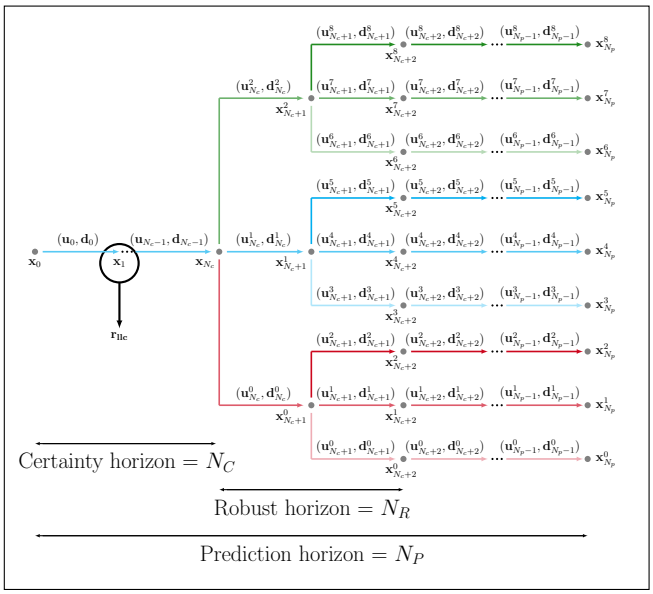

Fig. 2. A schematic of the modified multi-stage economic nonlinear model predictive used for reference generation. x_1 is a reference for some low-level controller (llc).

The NLP in (10) that describes the CE-ENMPC is computed every step before being shifted forward in time and recomputed. The disturbance vector $\widehat{d}_k$ is considered in the NLP as the *conditional expected* disturbance vector forward in time, and a correction is applied at the next time step.

B. Proposed controller - Multi-Stage approach

The multi-stage variant computes its control actions, analogous to the CE-ENMPC, by predicting x_{k+1}, which are optimised $\forall k = [0, N_P]$ before being shifted to the next time step and recomputed. The difference between an M-ENMPC and a CE-ENMPC lies in the handling of the uncertain disturbances $\widehat{d}$, which are addressed by constructing a scenario tree with discrete representative scenarios to represent some probability distribution, see Fig. 2. Fig. 2 illustrates the scenario tree which the M-ENMPC most commonly employs, which is based on three branches to account for the nominal d^1, the minimum d^0, and the maximum d^2 realisation of $\widehat{d}$. The optimal control input is then computed according to an expected value formulation.

In some power systems applications, forecasting can enhance the controller for better performance [17]. This paper extends forecasting for the M-ENMPC by imposing a certainty horizon N_C to exploit forecasting information, which is often accurate for a short time horizon, see Fig. 2. After N_C, the M-ENMPC used in this paper follows the nominal form where the amount of times branching occurs follows a robust horizon N_R formulation for tractability and prediction horizon N_P is the same as for the CE-ENMPC [9]. As the branching occurs much later, a decrease in computational cost can be achieved due to reducing decision variables in the NLP, thereby improving numerical tractability. Additionally, it becomes trivial to compute the references in the following step state predictions x_1 using the modified M-ENMPC as x_1 can be chosen similar to the CE-ENMPC, see Fig. 2. In

contrast, it is non-trivial to decide between the nominal, the minimum, or the maximum optimal state prediction in the nominal formulation of the M-ENMPC from [9] as branching occurs already at the initial node x_0 (unless the references in questions are the input u_0).

The resulting control problem can be formulated according to (10) during the certainty horizon, which thereafter assumes a scenario tree representation, where each next state x^i_{k+1} at stage $k+1$ after N_C and position i in the tree depends on the parent state x^i_k at stage k and the corresponding input u^i_k and current realisation of the disturbance d^i_k. If one defines the set of indices (i,k) in the scenario tree as $\boldsymbol{I}$ where $k \in [N_C+1, N_P]$ and $i \in [0, 3^{n_d} \cdot 3^{N_R-1}]$, then the following NLP solves the certainty-based M-ENMPC

$$
\begin{aligned}
\min_{x,u} \quad & J_{\text{ohps,multi}} + J_{\text{ohps,nominal}} \\
\text{subject to:} \quad & x_{k+1} = f\left(x_k, u_k, \widehat{d}_k\right),\ \forall k \in [0, N_C] \\
& h_{\text{ineq}}\left(x_k, u_k, \widehat{d}_k\right) \leq 0,\ \forall k \in [0, N_C] \\
& g_{\text{eq}}\left(x_k, u_k, \widehat{d}_k\right) = 0,\ \forall k \in [0, N_C] \\
& x^i_{k+1} = f\left(x^i_k, u^i_k, d^i_k\right),\ \forall (i,k) \in \boldsymbol{I} \\
& h_{\text{ineq}}\left(x^i_k, u^i_k, d^i_k\right) \leq 0,\ \forall (i,k) \in \boldsymbol{I} \\
& g_{\text{eq}}\left(x^i_k, u^i_k, d^i_k\right) = 0,\ \forall (i,k) \in \boldsymbol{I},
\end{aligned}
\tag{11}
$$

where $J_{\text{ohps,multi}} + J_{\text{ohps,nominal}}$ is defined as

$$
J_{\text{ohps,nominal}} = \sum_{k=0}^{N_C} J_{\text{ohps}}(x_k, u_k, d_k) \tag{12}
$$

$$
J_{\text{ohps,multi}} = \sum_{\forall (i,k) \in \boldsymbol{I}} J_{\text{ohps}}\left(x^i_k, u^i_k, d^i_k\right), \tag{13}
$$

with w^i_k being the probability of the different realisations of d. Additionally, non-anticipativity constraints on the form of

$$
0 \leq u^j_k - u^i_k \leq 0 \quad \text{if} \quad x^j_k = x^i_k,\ \forall (i,k) \in \boldsymbol{I}, \tag{14}
$$

are included in $h_{\text{k,ineq}}(\cdot)$ in addition to $h_{\text{ineq}}(\cdot)$ from [3] to model real-time decisions [18].

The M-ENMPC accounts for two uncertain variables in the case of the OHPS (v_{wind} and P_{demand}), resulting in $3^2 \cdot 3^{N_R-1}$ branches. As v_{wind} (in the form of P_{wtg}) and P_{demand} interact through (8) as a sum, a combined uncertain variable can instead be defined to simplify the M-ENMPC to only $3^1 \cdot 3^{N_R-1}$ branches instead of $3^2 \cdot 3^{N_R-1}$. Intuitively, this reduction is because a higher/lower P_{demand} and a lower/higher P_{wtg} have the same effect on the OHPS.

IV. SIMULATION STUDY

A simulation study is presented to validate the proposed method for reference optimisation of an OHPS in a case study with one lumped uncertain power consumer and uncertain wind power production. Including the uncertain demand side is essential as the trend goes toward decentralisation on the demand side, where demand forecasts may deviate from the actual demand [19]. Subsection IV-A first presents the simulation environment and variables used for the simulation study. Subsection IV-B follows by comparing the M-ENMPC to a CE-ENMPC for a single day. Thereafter, Subsection IV-C validates the results from Subsection IV-B for multiple realisations of uncertainty with 50 Monte Carlo simulations. Lastly, Subsection IV-D compares the modified M-ENMPC with the nominal one from [9]

A. Simulation Environment and Variables

A computer with an Intel(R) Core(TM) i7-9850H CPU @ 2.60 GHz is used to simulate the controllers for this study. The optimal control problems (OCPs) are formulated with CasADI [20], utilising a multiple shooting approach, and solved with IPOPT [21] using ma27 [22] as the linear solver.

Each simulation is run for 43200 s ($\approx$ 12 hours) with a time step of 30 s for each Monte-Carlo simulation. The methods are recomputed every time step with a prediction horizon of 3000 s. The methods are initialised with an initial system state $x_0 = [0.001,\ 0.001,\ 0.9,\ 0.001,\ 0.001]^\top$, with a prediction/control horizon of 100 time steps (= 3000 s).

It is assumed for simplicity that the plant and control models are identical, where $\alpha = [-1.59 \cdot 10^{-6}, 1.84 \cdot 10^{-2}]$, with full-state feedback and no process/measurement noise. The uncertainties arise from v_{wind} (which affects the P_{wtg} predictions through (1)) and P_{demand} forecast described by

$$
\text{v}_{\text{wind}} = A_{\text{v}_{\text{wind}}} \sin\left(\frac{1}{f_{\text{v}_{\text{wind}}}} t\right) + K_{\text{v}_{\text{wind}}} + w_{\text{v}_{\text{wind}}} \tag{15}
$$

$$
P_{\text{demand}} = w_{P_1} + w_{P_2}, \tag{16}
$$

and Table I. The power demand is a function of two random variables w_{P_i} that change their values every $T_{s,w_{P_i}}$ [s]. Similarly, the average wind rotor wind speed is defined for simplicity as a noisy sine curve using a Gaussian random variable $w_{\text{v}_{\text{wind}}}$ [23] that changes its value every $T_{s,w_{\text{v}_{\text{wind}}}}$.

TABLE I
WIND AND EXOGENOUS POWER DEMAND PARAMETERS

Symbol	Value	Symbol	Value
$w_{\text{v}_{\text{wind}}}$	$\mathcal{N}(0,1)$	w_{P_1}	$\mathcal{N}(0,500)$
$K_{v_{\text{wind}}}$	7.5	w_{P_2}	$\mathcal{U}(2000,8800)$
$A_{v_{\text{wind}}}, f_{v_{\text{wind}}}$	0.5,200	$T_{s,w_{P_1}}$	6000
$T_{s,w_{v_{\text{wind}}}}$	900	$T_{s,w_{P_2}}$	2250

By assuming that uncertainties are known accurately for the first 5 minutes, the certainty horizon for the M-ENMPC is N_C = 10 (the choice of N_C depends on the uncertainty, for wind data, 5 minutes is reasonable [24]), while a robust horizon N_R = 1 was adequate. The branches in the M-ENMPC are weighted by hand according to: $\omega^{\mathbf{i}}_{N_C+1} = [0.175, 0.65, 0.175]$ with $\mathbf{i} \in [0,2]$, where the maximum and minimum realisations of the combined uncertainty are set to $\pm 40\% \approx \left(\frac{\text{var}(w_{P_2})}{P_{\text{demand}}} + \frac{\text{var}(w_{v_{\text{wind}}})}{\text{v}_{\text{wind}}}\right) \cdot 100$.

The resulting references from the different methods (given by the following state prediction x_1 after the initial state x_0) are assumed to be followed perfectly by some low-level controllers. For comparison reasons, the tuning constants K_i in the cost function from Subsection II-B are kept the same for the different methods and weighted by hand according

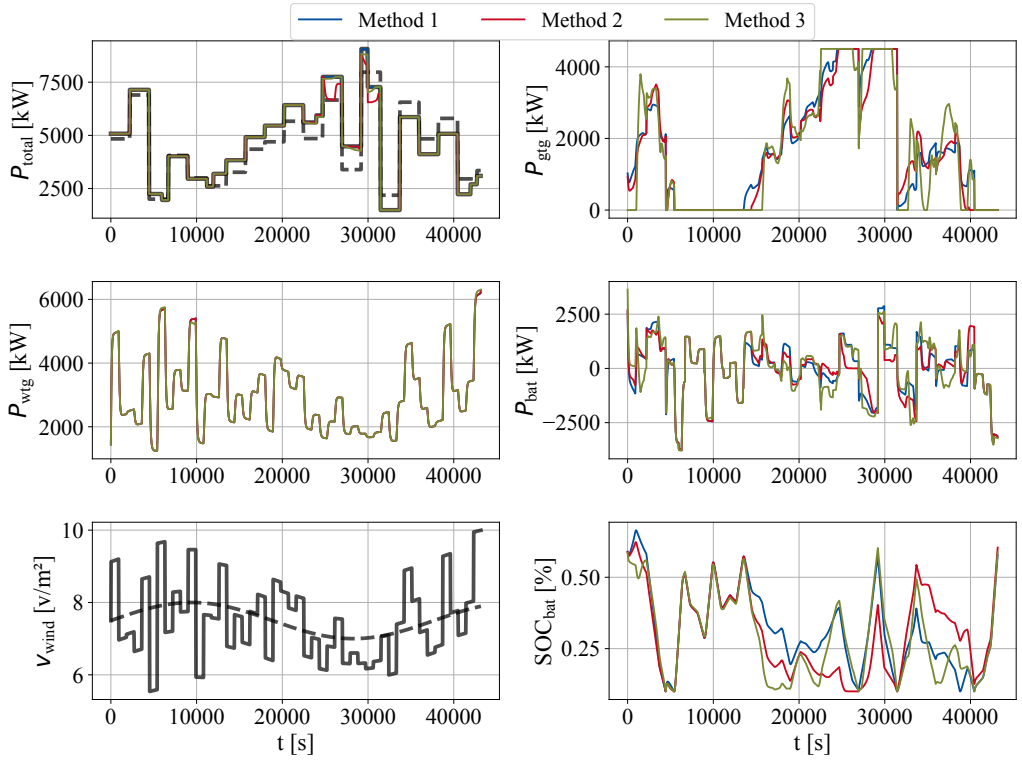

Fig. 3. Time profiles of the open-loop references for total power P_{total}, GTG power P_{gtg}, WTG power P_{wtg}, battery power P_{bat}, and battery state of charge SOC_{bat} references from the different methods, given current wind speed v_{wind}. Forecasts are colored in black, where stipulated black lines represent the imperfect forecasts of total power demand and wind. In contrast, solid black lines represent the realisation of wind and power demand.

to: $K_{\text{wtg}} = 10$, $K_{\text{gtg},\eta} = 5$, $K_{\text{gtg},P} = 200$, $K_{\text{bat}} = 1$, and $K_u = \text{diag}(1, 10000, 10)$.

Subsequently, the identifiers in Table II will be used for the different methods compared in this section, where the first identifier represents an upper bound on the performance as this method employs the CE-ENMPC with perfect forecasts of the wind ($w_{\text{v}_{\text{wind}}}$) and exogenous power demand (w_{P_1},w_{P_2}). Identifier 2 represents what can be achieved given imperfect forecasts $(w_{\text{v}_{\text{wind}}}, w_{P_1}) = (0, 0)$ using a CE-ENMPC. Finally, identifier 3 is used for the certainty-horizon-based M-ENMPC given imperfect forecasts. In practice, only imperfect knowledge of these forecasts is realistic. Lastly, identifier 4 is used for the nominal M-ENMPC from [9]. For a fair comparison, method 2 and 4 also uses a certainty horizon scheme where the disturbances are known accurately (however, method 4 still branches at the initial node where the nominal trajectory is used as the next reference value).

TABLE II

IDENTIFIERS FOR THE METHODS TO BE COMPARED

Identifier	Method
1	CE-ENMPC with perfect forecasts
2	CE-ENMPC with imperfect forecasts
3	Modified M-ENMPC with imperfect forecasts
4	Nominal M-ENMPC with imperfect forecasts

B. Single Day Case Simulation

The proposed methods (excluding 4) are initially compared for a single simulation of 12 hours to understand the qualitative differences. Fig. 3 shows the results of applying the different methods for reference optimisation of an OHPS for a single simulation. For simplicity, only the power responses P for the GTG, the WTG, and the battery are shown (where $P_{\text{total}} = P_{\text{gtg}} + P_{\text{wtg}} + P_{\text{bat}}$), including the average WTG rotor wind speed v_{wind} and the battery state of charge SOC_{bat}.

As expected, method 1, with perfect forecasts of v_{wind} and P_{demand}, satisfies the power demand P_{demand} completely. Method 2 performs the worst in terms of satisfying P_{demand} due to imperfect forecasting. The lack of precise forecasting affects how much in advance the methods can preemptively charge the battery SOC when required. Most notable, the state around $t = 29000$ s shows a particularly demanding scenario for the system as the total power demand cannot be satisfied by P_{wtg} and the maximum gas turbine power output $P_{\text{gtg,max}}$ ($P_{\text{wtg,t=29000}} + P_{\text{gtg,max}} \leq P_{\text{demand,t=29000}}$), the OHPS thus needs to charge the battery using the gas turbine preemptively, which is only possible with accurate forecasting.

A closer look at Fig. 3 shows that method 3 achieves an acceptable degree of satisfaction of the total power demand P_{demand}. At around t = 16000 s, method 3 has a much lower reference for the battery storage SOC_{bat} compared to the other methods while still being able to charge the battery at t = 29000 s sufficiently. This is due to how branching is implemented in the M-ENMPC, which accounts for the maximum and minimum realisations of uncertain disturbances. By accounting for the uncertainties, method 3 accounts for the lowest possible wind power output $P_{\text{wtg,lowest}}$ (where $P_{\text{wtg,lowest}} \leq P_{\text{wtg,nominal}} \leq P_{\text{wtg,highest}}$) and the highest possible power demand $P_{\text{demand,highest}}$ (where $P_{\text{demand,lowest}} \leq$

$P_{\text{demand,nominal}} \leq P_{\text{demand,highest}}$). Since $P_{\text{demand,highest,t=16000}} \leq P_{\text{wtg,lowest,t=16000}} + P_{\text{gtg,max}}$ at t = 16000 s, method 3 is free to empty the battery and still be able to satisfy P_{demand}, given that the minimum and maximum values are sufficiently accurate. Conversely, this also translates to how method 3 manages to preemptively charge the battery at t = 29000 s. An automatic back-off in (8) is introduced in the NLP as method 3 accounts for $P_{\text{wtg,lowest}}$ and $P_{\text{demand,highest}}$. Method 3 therefore charges the battery at t = 29000 s, since $P_{\text{wtg,lowest,t=29000}} + P_{\text{gtg,max}} \leq P_{\text{demand,highest,t=29000}}$.

Table III summarises the results by highlighting the key performance indicators (KPIs), where $P_{\text{error}} = P_{\text{demand}} - (P_{\text{wtg}} + P_{\text{gtg}} + P_{\text{bat}})$. A closer look at Table III (where all of the KPIs are summed for the whole simulation duration except for the efficiency η_{gtg}, which is averaged) shows that method 3 achieves an increased η_{gtg} which results in lower GHG emissions even compared to the benchmark method 1.

The increased gas turbine efficiency of method 3 can be attributed to how uncertainty is explicitly defined in the optimisation problem. As method 3 accounts for $P_{\text{wtg,lowest}}$ and $P_{\text{demand,highest}}$, it can optimise the references based on the control input which will improve performance for all considered scenarios. For example, at t = 16000 s, the battery is fully discharged method 3. The effect of running the battery dry is that it later can, on average, increase the gas turbine power output, thus increasing the turbine's efficiency, see (7). In this case, method 3 already accounts for an overestimation of the power demand and an underestimation of the wind power output and also optimises for these scenarios. In contrast, methods 1 and 2 do not consider uncertainty and aim to precisely satisfy the power demand for the nominal branch. As such, optimality for methods 1 and 2 is achieved by jointly satisfying the power demand with both the battery and the gas turbine at partial load.

TABLE III

KEY PERFORMANCE INDICATORS FOR SINGLE DAY CASE.

Method	P_{error} [MW]	$\bar{\eta}_{gtg}$[%]	P_{gtg} [GW]	GHG [Mg CO_2]
1	23.76	31.21	75.19	12.30
2	2954.37	32.15	72.43	11.62
3	794.85	36.48	74.55	10.65

C. Monte Carlo Simulations

50 Monte-Carlo simulations for each of the compared methods are simulated for each uncertain disturbances (v_{wind} and P_{wtg}) to draw statistical conclusions and confirm the results from the single case simulation in Fig. 3. The results are summarised in Fig. 4, which uses box plots to compare the four KPIs for the different methods.

As shown, Fig. 4 confirms the results of Subsection IV-B: On average, the M-ENMPC (in green) is an improvement over the CE-ENMPC with both perfect (in blue) and imperfect (in red) forecasts in terms of GHG emissions ($\text{GHG}_{\text{method 3}} \leq \text{GHG}_{\text{method 2}} \leq \text{GHG}_{\text{method 1}}$), while still achieving acceptable P_{error} relative to the CE-ENMPC ($P_{\text{error,method 1}} \leq P_{\text{error,method 3}} \leq P_{\text{error,method 2}}$). The gas turbine generator is used more often in method 3 compared to method 2, but the emitted GHG is lowest due to the increased efficiency.

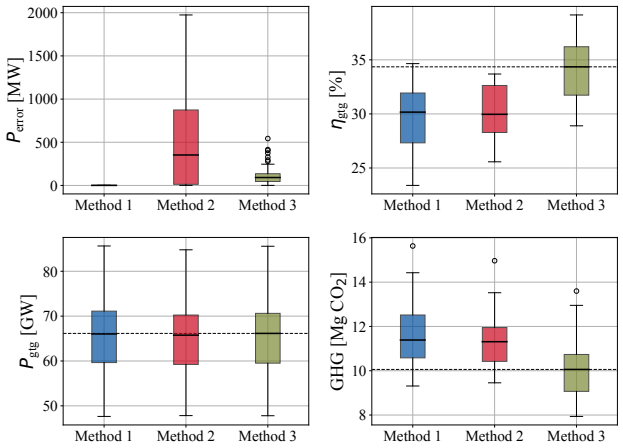

Fig. 4. Comparison results from the Monte Carlo simulations for methods 1-3. The key performance indicators are represented as box plots. A stipulated gray line is included for ease of comparison, while outliers are represented as circles.

D. Comparing nominal to modified multi-stage

Lastly, comparing the proposed method 3 against method 4 from the literature is essential. For that, the average computational cost of the different methods is computed by averaging the computational cost of each method over 50 Monte Carlo simulations. The results are listed in Table IV and show that, on average, method 3 decreases the average computational cost of each iteration by 17%.

TABLE IV

AVERAGE COMPUTATIONAL COST OF FULLY SOLVING THE DIFFERENT METHODS AT EACH TIME STEP.

Method 1	Method 2	Method 3	Method 4
0.11 s	0.11 s	0.39 s	0.47 s

Simulating method 4 over 50 Monte Carlo simulations results in Fig 5 shows that, on average, method 4 performs better than method 3. Most notably, method 4 performs better in terms of η_{gtg} and GHG. The increase in performance is because method 4 possesses more degrees of freedom during optimisation as it branches at the initial node compared to method 3, which branches after the certainty horizon. In many applications, this tradeoff between performance and computational cost is acceptable, as the computational cost of M-ENMPC prohibits many of its uses.

V. CONCLUDING REMARK

This paper proposes a certainty-horizon-based M-ENMPC for reference optimisation, given uncertain forecasting. The method is applied to an OHPS. However, the method can be extended to any control system utilising a CE-ENMPC for reference generation with uncertain forecasts. The proposed certainty-horizon-based M-ENMPC is validated in simulation with 50 Monte Carlo simulations and compared with a CE-ENMPC with perfect and imperfect forecasts of v_{wind} and P_{demand}. Simulations show that the M-ENMPC with imperfect forecasts can have increased performance when it comes to satisfying the uncertain exogenous power demand

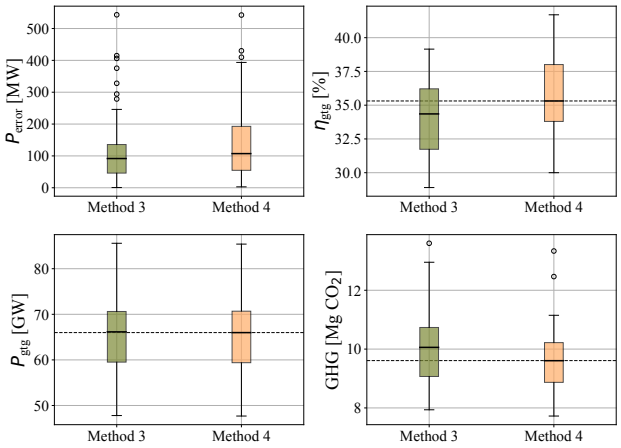

Fig. 5. Comparison results from the Monte Carlo simulations for methods 3-4. The key performance indicators are represented as box plots. A stipulated gray line is included for ease of comparison, while outliers are represented as circles.

compared to the CE-ENMPC with imperfect forecasts. Furthermore, a decrease in GHG emissions can be achieved with the M-ENMPC with imperfect forecasts even compared to the CE-ENMPC with perfect forecasts.

VI. FURTHER WORKS

Further work is required as the present method is tuned empirically and assumes constant parameters in the PDFs from which v_{wind} and P_{demand} are sampled. Considering PDFs where parameters such as the mean and variance (if one assumes white noise) are essential for the OHPS. For example, the P_{demand} fluctuates more during the day as there is naturally more activity, while v_{wind} fluctuates depending on factors such as season, day/night, location, and temperature. Techniques for this exists, for example [25] and [26].

Additionally, further work should investigate the optimality of using a certainty horizon based M-ENMPC compared to the nominal M-ENMPC formulation. It would be interesting to see whether branching at the beginning would result in vastly different state trajectories, even if the first predictions in each branch in the nominal M-ENMPC utilise the actual forecasts. Maybe even more interesting is to investigate the effect of the certainty horizon N_C on the expected performance. Further work should also investigate the trade-off between computational cost and performance on other applications, as the computational cost of the M-ENMPC prohibits its use in many applications.

REFERENCES

[1] W. Findeisen, F.N. Bailey, M. Brdys, K. Malinowski, P. Tatjewski, and A. Wozniak, Control and coordination in hierarchical systems. Wiley, 1980.

[2] X. Kong, X. Liu, L. Ma, and K.Y. Lee, Hierarchical Distributed Model Predictive Control of Standalone Wind/Solar/Battery Power System, in IEEE Transactions on Systems, Man, and Cybernetics: Systems, vol. 49, no. 8, pp. 1570-1581, 2019.

[3] K.T. Hoang, B.R. Knudsen, and L. Imsland, Hierarchical nonlinear model predictive control of offshore hybrid power systems, IFAC-PapersOnLine, vol 55, issue 7, pp 470-476, 2022.

[4] T. Marlin and A. Hrymak. Real-time operations optimization of continuous processes. AIChE Symp Ser CPC vol 93, 01, 1997

[5] L. Wurth, R. Hannemann, and W. Marquardt. A two-layer architecture for economically optimal process control and operation. Journal of Process Control, 21(3):311–321, 2011.

[6] R. Scattolini, Architectures for distributed and hierarchical model predictive control, Journal of Process Control, pp. 723–731, 2009.

[7] A. Bemporad and M. Morari. Robust model predictive control: A survey. In: Garulli A., Tesi A. (eds) Robustness in identification and control. Lecture Notes in Control and Information Sciences, vol 245. Springer, London, 2007.

[8] A. Mesbah, Stochastic Model Predictive Control: An Overview and Perspectives for Future Research, in IEEE Control Systems Magazine, vol. 36, no. 6, pp. 30-44, 2016.

[9] S. Lucia, T. Finkler, and S. Engell, Multi-stage nonlinear model predictive control applied to a semi-batch polymerization reactor under uncertainty, Journal of Process Control, vol 23, issue 9, pp 1306-1319, 2013.

[10] J. Liu, P. Jayakumar, J.L. Stein, and T. Ersal. A Multi-Stage Optimization Formulation for MPC-Based Obstacle Avoidance in Autonomous Vehicles Using a LIDAR Sensor. Proceedings of the ASME 2014 Dynamic Systems and Control Conference, V002T30A006, 2014.

[11] D. Krishnamoorthy, B. Foss, and S. Skogestad, Gas Lift Optimization under Uncertainty, Computer Aided Chemical Engineering, vol 40, pp 1753-1758, 2017.

[12] Norwegian Petroleum Directorate. Resource Report, 2019

[13] H. Zhang, A. Tomasgard, B.R. Knudsen, H.G. Svendsen, S.J.Bakker, and I.E.Grossmann, Modelling and analysis of offshore energy hubs, Energy, vol 261, part A, 2022.

[14] W. Nirbito, M.A. Budiyanto, and R. Muliadi. Performance Analysis of Combined Cycle with Air Breathing Derivative Gas Turbine, Heat Recovery Steam Generator, and Steam Turbine as LNG Tanker Main Engine Propulsion System. J. Mar. Sci. Eng, 8, 726, 2020.

[15] van de Water H, J. Willems, The certainty equivalence property in stochastic control theory. IEEE Transactions on Automatic Control, 26(5):1080 – 1087, 1981.

[16] J. Rawlings, D.Q. Mayne, and M. Diehl. Model Predictive Control: Theory, Computation, and Design.

[17] D. Bilgic, A. Koch, G. Pan, and T. Faulwasser, Toward data-driven predictive control of multi-energy distribution systems, Electric Power Systems Research, vol 212, 2022.

[18] J.R. Birge and F. Louveaux. Introduction to Stochastic Programming. Springer. 1997.

[19] S. Williams and M. Short, Electricity demand forecasting for decentralised energy management, Energy and Built Environment, vol 1, issue 2, pp 178-186, 2020.

[20] J.A.E. Andersson, J. Gillis, G. Horn, J. Rawlings, and M. Diehl. CasADi – A software framework for non-linear optimization and optimal control. Mathematical Programming Computation, 11(1):1–36, 2019.

[21] A. Wächter and L. Biegler. On the implementation of an interior-point filter line-search algorithm for large-scale nonlinear programming.Mathematical programming,106:25–57, 03 2006.

[22] HSL. A collection of Fortran codes for large scale scientific computation, http://www.hsl.rl.ac.uk/.

[23] Lange, M. On the Uncertainty of Wind Power Predictions—Analysis of the Forecast Accuracy and Statistical Distribution of Errors. Journal of Solar Energy Engineering-transactions of The Asme - J SOL ENERGY ENG. 127. 10.1115/1.1862266, 2005.

[24] L. Xie et al, Wind Integration in Power Systems: Operational Challenges and Possible Solutions, in Proceedings of the IEEE, vol. 99, no. 1, pp. 214-232, 2011.

[25] F. Holtorf, A. Mitsos, and L.T. Biegler, Multistage NMPC with on-line generated scenario trees: Application to a semi-batch polymerization process, Journal of Process Control, vol 80, pp 167-179, 2019.

[26] A.D. Bonzanini, J.A. Paulson, G. Makrygiorgos, and A. Mesbah, Fast approximate learning-based multistage nonlinear model predictive control using Gaussian processes and deep neural networks, Computers & Chemical Engineering, vol 145, 2021.